*Proc. Natl. Acad. Sci. USA*
Vol. 92, pp. 4492–4496, May 1995
Developmental Biology

# Gain of function mutations for paralogous *Hox* genes: Implications for the evolution of *Hox* gene function

(atavism/paralog/skeleton/transgenic mice)

ROBERT A. POLLOCK, TADURU SREENATH, LIEN NGO, AND CHARLES J. BIEBERICH

Department of Virology, Jerome H. Holland Laboratory, 15601 Crabbs Branch Way, Rockville, MD 20855

*Communicated by Frank H. Ruddle, Yale University, New Haven, CT, January 3, 1995*

**ABSTRACT** **To investigate the functions of paralogous *Hox* genes, we compared the phenotypic consequences of altering the embryonic patterns of expression of *Hoxb-8* and *Hoxc-8* in transgenic mice. A comparison of the phenotypic consequences of altered expression of the two paralogs in the axial skeletons of newborns revealed an array of common transformations as well as morphological changes unique to each gene. Divergence of function of the two paralogs was clearly evident in costal derivatives, where increased expression of the two genes affected opposite ends of the ribs. Many of the morphological consequences of expanding the mesodermal domain and magnitude of expression of either gene were atavistic, inducing the transformation of axial skeletal structures from a modern to an earlier evolutionary form. We propose that regional specialization of the vertebral column has been driven by regionalization of *Hox* gene function and that a major aspect of this evolutionary progression may have been restriction of *Hox* gene expression.**

The *Drosophila* homeotic complex (*Hom-C*) encodes a family of regionally expressed transcriptional regulators that are largely responsible for establishing the identity of individual body segments. Homologs of *Hom-C* genes are present in the genome of many metazoans, raising the possibility that this gene family represents a conserved genetic system that provides positional information central to the development of a wide variety of body plans (reviewed in ref. 1).

In the chordate lineage, the expansion and duplication of a primordial gene cluster has given rise to four mammalian *Hox* clusters (2), which in mice are termed *Hoxa*, *Hoxb*, *Hoxc*, and *Hoxd* (3). Mouse and human *Hox* genes can be arranged into 13 paralogous groups based on amino acid sequence similarity and position within each cluster (4–6). It has been suggested that duplication of clusters has provided the developmental capacity to evolve increasingly complex body plans (5, 7). This view predicts that duplicated genes would functionally diverge to provide the plasticity necessary for increased morphological complexity. Experimental evidence in support of this hypothesis has emerged from recent loss of function analyses of paralogous *Hox* genes (22). In the present study, the opposite strategy, a gain of function approach, is used to investigate the functions of medial group paralogous *Hox* genes. The data reported here are consistent with a causal link between expansion of the *Hox* gene family and evolution of the vertebrate body plan but further suggest that regional loss of *Hox* gene function has also played an important role in this process.

## MATERIALS AND METHODS

To compare the phenotypic consequences of altered *Hoxc-8* expression with its paralog *Hoxb-8*, we derived a *Hoxb-8* transgene with a pattern of expression that would precisely parallel that previously described for the *Hoxc-8* transgene (termed here $Hox^{a\text{-}4}c\text{-}8$) (8) driven by a transcriptional control region of *Hoxa-4* (9). The $Hox^{a\text{-}4}b\text{-}8$ transgene was generated by ligation of a 4.8-kb *Kpn* I/*Apa* I fragment and a 4.1-kb *Kpn* I/*Sac* I fragment from plasmid $pHox^{a\text{-}4}c\text{-}8$ (designated p14/31 in ref. 8) with an 861-bp *Sac* I/*Apa* I fragment containing the *Hoxb-8* protein coding sequence derived by reverse transcriptase PCR using the *Hoxb-8* primers 5′-caataaaatgagctcttatttcgtc-3′ and 5′-cggacgtgcgggctagtc-3′. A single nucleotide difference was found at position 228 of the *Hoxb-8* coding sequence obtained from FVB cDNA compared to the reported *Hoxb-8* coding sequence (10) that would result in an alanine to glycine substitution 19 amino acids carboxyl to the homeodomain. Since it was not clear whether this conservative substitution represented a mutation introduced during cloning or a genuine polymorphism, two versions of the transgene were constructed containing either glycine or alanine at position 228. Indistinguishable results were obtained with the two sequences, and four specimens included in Table 1 contain the glycine 228 version of the transgene. The transgene construct was digested with *Xho* I and *Kpn* I to release a 6.9-kb insert, which was injected into FVB embryos. DNA from founder generation pups was digested with *Eco*RI and *Pst* I and probed with a 440-bp *Apa* I/*Eco*RI fragment from $pHox^{a\text{-}4}b\text{-}8$ in a Southern blot analysis.

*In situ* hybridization was performed as described (11) with the oligonucleotides 5′-gaaagaattacggcgtgaataggcagtttcatgttgttgg-3′ and 5′-accttctcctcatctcgggcccgagcagtcccag-3′ to detect the endogenous and transgenic *Hoxb-8* mRNAs, respectively.

## RESULTS

**Analyses of Transgene Expression.** *In situ* hybridization of serial sections of 12.5-days postcoitus (p.c.) $Hox^{a\text{-}4}b\text{-}8$ embryos and their nontransgenic littermates with a transgene-specific probe revealed signal only in the transgenic embryos (Fig. 1 *A* and *C*). Transgene expression was observed in the developing spinal cord with an anterior boundary in the roof of the myelencephalon (Fig. 1*A*), 1–2 mm anterior of the rostral limit of expression of the endogenous *Hoxb-8* gene (Fig. 1*B*). In the developing axial skeleton, transgene expression was observed from prevertebrae (pv) 8 to pv27 and was detected in developing centra, neural arches, intervertebral disk anlagen, and throughout the proximodistal axis of ribs. $Hox^{a\text{-}4}b\text{-}8$ mRNA was also evident in lungs, kidneys, stomach, and intestine. The pattern of expression of the $Hox^{a\text{-}4}b\text{-}8$ transgene reported here is essentially identical with that reported for the $Hox^{a\text{-}4}c\text{-}8$ transgene (8). Although the pattern of expression of $Hox^{a\text{-}4}c\text{-}8$ and $Hox^{a\text{-}4}b\text{-}8$ closely parallels that reported for the *Hoxa-4* promoter (9) in most tissues, expression in paraxial mesoderm diverges from the predicted pattern, a fact that could reflect interaction between *Hoxa-4* upstream transcriptional control elements and *Hoxc-8* elements located in the 3′ nontranslated region of both constructs (8).

The publication costs of this article were defrayed in part by page charge payment. This article must therefore be hereby marked "*advertisement*" in accordance with 18 U.S.C. §1734 solely to indicate this fact.

Abbreviations: p.c., postcoitus; pv, prevertebra(e).

Table 1. Costovertebral markers in normal and transgenic skeletons

| | | *Hox$^{a\text{-}4}$b-8* | | *Hox$^{a\text{-}4}$c-8* | | FVB | |
|---|---|---|---|---|---|---|---|
| | | L | R | L | R | L | R |
| Transitional vertebra | T10 | 4/9 | 4/9 | 3/19 | 2/19 | 110/110 | 110/110 |
| | T11 | 5/9 | 4/9 | 11/19 | 9/19 | 0/110 | 0/110 |
| | T12 | 0/9 | 1/9 | 5/19 | 8/19 | 0/110 | 0/110 |
| Thoracic transverse process | T10 | 9/9 | 9/9 | 19/19 | 19/19 | 110/110 | 110/110 |
| | T11 | 7/9 | 6/9 | 15/19 | 15/19 | 0/110 | 0/110 |
| | T12 | 1/9 | 1/9 | 5/19 | 4/19 | 0/110 | 0/110 |
| Costal tubercle | R10 | 9/9 | 9/9 | 19/19 | 19/19 | 106/110 | 106/110 |
| | R11 | 2/9 | 4/9 | 13/19 | 16/19 | 0/110 | 1/110 |
| | R12 | 1/9 | 1/9 | 11/19 | 11/19 | 0/110 | 0/110 |
| | R13 | 1/9 | 1/9 | 1/19 | 3/19 | 0/110 | 0/110 |
| 8 VS ribs | | 0/9 | 1/9 | **7/16** | **9/17** | 1/142 | 2/142 |
| Malformed sternebrae | | 0/9 | | **8/16** | | 10/142 | |
| Supernumerary ribs* | L1 | 8/9 | 9/9 | 13/19 | 14/19 | 1/162 | 0/162 |
| | L2 | **4/9** | **4/9** | 0/19 | 0/19 | 0/162 | 0/162 |
| | L3 | **2/9** | **3/9** | 0/19 | 0/19 | 0/162 | 0/162 |
| | L4 | 0/9 | **1/9** | 0/19 | 0/19 | 0/162 | 0/162 |
| | L5 | 0/9 | 0/9 | 0/19 | 0/19 | 0/162 | 0/162 |
| Rib-like pleurapophyses | L1 | 0/9 | 0/9 | 0/19 | 0/19 | 0/64 | 0/64 |
| | L2 | 0/9 | 0/9 | 0/19 | 0/19 | 0/64 | 0/64 |
| | L3 | **3/9** | **2/9** | 0/19 | 0/19 | 0/64 | 0/64 |
| | L4 | **3/9** | **1/9** | 0/19 | 0/19 | 0/64 | 0/64 |
| | L5 | **4/9** | **3/9** | 0/19 | 0/19 | 0/64 | 0/64 |
| | L6 | **4/9** | **3/9** | 0/19 | 0/19 | 0/64 | 0/64 |
| Rib shaft exostoses† | | **6/9** | | 0/19 | | 0/64 | |
| Rib head exostoses† | | **6/9** | | 0/19 | | 0/64 | |
| Malformed centra† | | **4/9** | | 0/19 | | 0/64 | |

Boldface lettering indicates alterations unique to either transgene. Where appropriate, left (L) and right (R) sides of each animal were scored independently. Nine of 10 *Hox$^{a\text{-}4}$b-8* founder neonates exhibited altered skeletal morphology for the markers indicated. *Hox$^{a\text{-}4}$c-8* data represent newborn pups from three established lines and 5 of 8 founder neonates. Three apparently normal founders were not included. VS, vertebrosternal.

*Costal structures having an ossified shaft and a cartilaginous head that articulates with a vertebra.

†Total number of animals bearing this marker is indicated.

Analyses of sections from transgenic and nontransgenic embryos revealed identical patterns of expression of the endogenous *Hoxb-8* gene (Fig. 1 *B* and *D*). The *Hoxb-8* transcript was detected in all spinal ganglia and from the roof of the myelencephalon to a posterior border close to the tip of the tail in the central nervous system (Fig. 1 *B* and *D*), in agreement with the expected pattern of *Hoxb-8* expression (12, 13). *Hoxb-8* mRNA was also detected in pv8 to pv20. This rostral limit is one segment more posterior than that reported for *Hoxb-8* in 11.5-day p.c. embryos (13), a finding that may reflect either a decrease in expression to a level below detectable limits in pv7 at 12.5 days p.c. or differences in threshold sensitivity in the two studies. The highest levels of prevertebral expression were detected over pv9 to pv16 (Fig. 1 *B* and *D*), and expression was not evident above background posterior to pv20 to pv21. Expression was also detected in loose mesenchyme between ribs and the proximal portion of ribs including the presumptive rib head, neck, and tubercle (Fig. 1 *E* and *F*).

**Transformations Common to Increased Expression of *Hoxb-8* and *Hoxc-8*.** Examination of axial skeletons of *Hox$^{a\text{-}4}$b-8* and *Hox$^{a\text{-}4}$c-8* transgenic newborns revealed homeotic transformations (14) common to expression of both transgenes

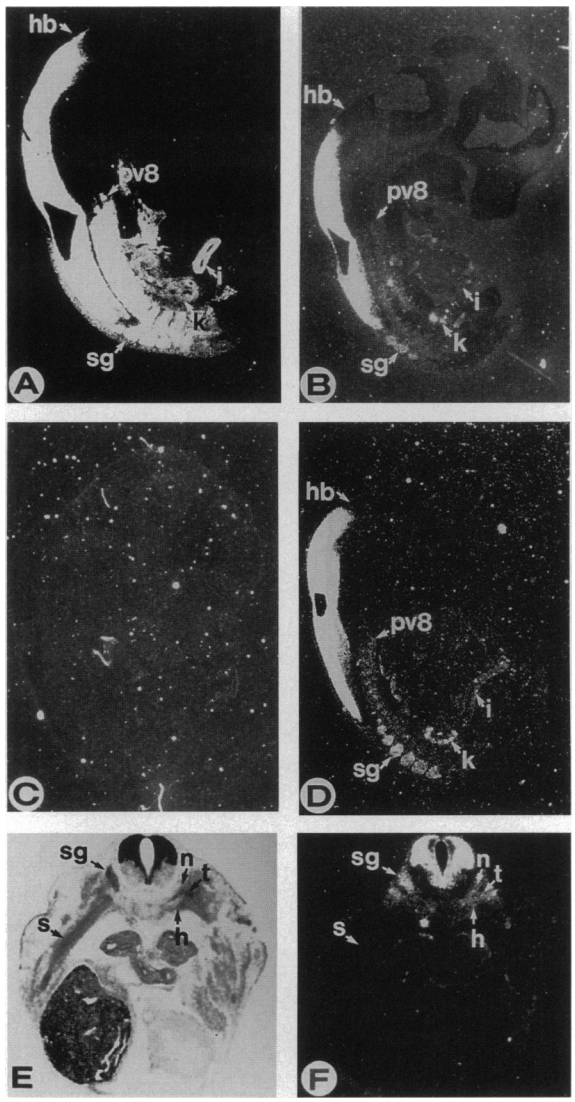


FIG. 1. Dark-field views of near midsagittal serial sections of a 12.5-day p.c. *Hox$^{a\text{-}4}$b-8* embryo hybridized with a probe specific for (*A*) transgene mRNA and (*B*) endogenous *Hoxb-8* mRNA. Dark-field views of near midsagittal serial sections of a 12.5-day p.c. FVB embryo hybridized with a probe specific for transgene mRNA (*C*) and endogenous *Hoxb-8* mRNA (*D*). Bright-field (*E*) and dark-field (*F*) view of a cross-section from the thoracic region of a 12.5-day p.c. FVB embryo hybridized with a probe specific for the endogenous *Hoxb-8* mRNA. hb, Hindbrain; pv8, centrum of pv8; sg, spinal ganglia; k, kidney; i, intestine; n, neural arch; t, rib tubercle; h, rib head; s, rib shaft.

(Table 1). Most notably, the pattern of articulation between neural arches of successive thoracic vertebrae was substantially altered in both sets of transgenic mice. The point along the vertebral column at which the type of articulation between neural arches switches from an anterior form capable of a wide range of motion to a more restrictive posterior type is called the transitional vertebra and is invariably found at the 10th thoracic vertebra (T10) in FVB mice (Fig. 2*A*; Table 1; ref. 8 and references therein). In both *Hox$^{a\text{-}4}$b-8* and *Hox$^{a\text{-}4}$c-8* transgenic mice, the transitional vertebra was usually observed at T11 or T12 (Fig. 2 *B* and *C*; Table 1) concomitant with a posterior shift in the position of the transverse process. The presence of either transgene resulted in the appearance of ribs or rib anlagen on the first lumbar vertebra (L1) (Fig. 3 *E* and *F*; Table 1) and the appearance of costal tubercles on ribs 11–13 (Table 1).

**Morphologic Alterations Specific to *Hox$^{a\text{-}4}$b-8* Mice.** Phenotypic consequences of *Hoxb-8* overexpression were observed in the region spanning T2 through L6. Most evident in the

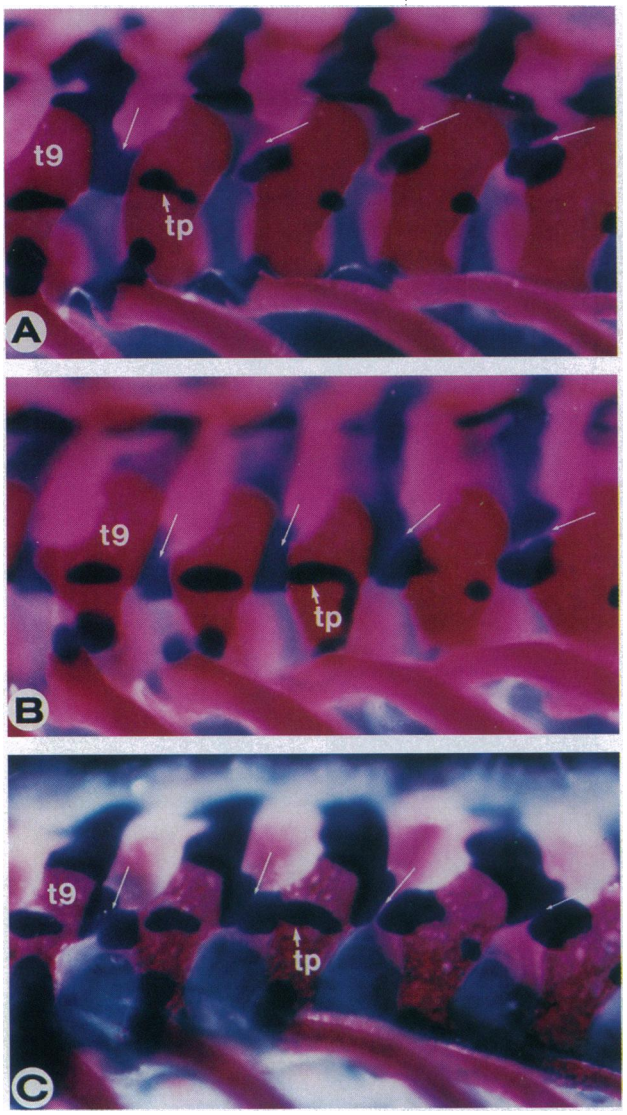


FIG. 2. (*A*) Lateral view of ribs and neural arches of an FVB mouse illustrates that T10 bears the most posterior transverse process (tp) and is the transitional vertebra. *Hox$^{a\text{-}4}$b-8* (*B*) and *Hox$^{a\text{-}4}$c-8* (*C*) specimens both show transverse processes and transitional vertebrae at T11. The transitional vertebra marks the position of a dramatic change in the pattern of articulation between adjacent neural arches. While this is in fact a complex three-dimensional alteration, the overall angle of articulation change has been approximated here by the inclination of white arrows. t9, Neural arch of the ninth thoracic vertebra.

thoracic region were alterations in rib morphology, particularly ribs 6–12 (i.e., Fig. 3*B* and Table 1). Rib heads and the proximal ends of the shafts were grossly enlarged and in several instances were clearly bifurcated (Fig. 3*B*). Prominent epiphyseal exostoses involving rib head cartilage were present in the costovertebral joints of 6/9 *Hox$^{a\text{-}4}$b-8* animals (Fig. 3*B*).

Branching of rib shafts was also observed in 6/9 *Hox$^{a\text{-}4}$b-8* newborns (Table 1). These protuberances consisted of an ossified base with a cartilaginous cap and were morphologically similar to rib heads or tubercles and could be considered ectopic examples of these structures. Ectopic rib heads were confined to the proximal third of the rib and resulted in the inappropriate articulation of adjacent rib heads, of rib heads with adjacent shafts, or of neighboring shafts (Fig. 3*B*). Costal cartilages at the distal ends of the ribs were unaffected in *Hox$^{a\text{-}4}$b-8* transgenic mice (Table 1).

In *Hox$^{a\text{-}4}$b-8* transgenic mice, lumbar ribs could be seen as far posterior as L4 (Table 1; Fig. 3*E*). Ribs found on L2–L4 consisted of a cartilaginous head with a short ossified shaft completely lacking cartilage at the distal end of the shaft (Fig. 3*E*). These lumbar ribs could project laterally or even anteriorly and in all cases coincided with the absence of a lumbar transverse process termed the pleurapophysis (15).

The pleurapophysis is a forward-pointing process that projects from the ventrolateral aspect of the neural arch of all lumbar and some caudal vertebrae. This structure is rudimentary on L1 but becomes progressively more prominent posteriorly, where adjacent pleurapophyses fuse to form the sacrum. Pleurapophyses of FVB mice are cartilaginous at birth and ossify in a proximodistal manner over the first 2 weeks of neonatal life (R.A.P., unpublished data). In contrast, lumbar pleurapophyses of *Hox$^{a\text{-}4}$b-8* mice were precociously calcified at the time of birth and ossified from the center of the cartilaginous process in a manner analogous to that of a rib shaft. This aberrant pattern of ossification was invariably associated with the appearance of a cartilaginous projection into the intervertebral space at the base of the process, in precisely the position and orientation expected for a rib head (Fig. 3*E*). In addition to costal alterations, asymmetric ossification of vertebral centra was evident in the thoracic region of 4/9 *Hox$^{a\text{-}4}$b-8* transgenic mice (Fig. 3*B*; Table 1).

**Morphologic Changes Specific to Overexpression of *Hoxc-8*.** Morphologic alterations observed exclusively in *Hox$^{a\text{-}4}$c-8* transgenic mice were confined to distal ends of ribs and the sternum. Whereas 98% of FVB mice have seven vertebrosternal ribs, 50% of the *Hox$^{a\text{-}4}$c-8* mice had at least one additional rib fused to the sternum (Table 1). *Hox$^{a\text{-}4}$c-8* mice frequently showed altered ossification of the sternebrae resulting in a crankshaft pattern. Since sternebrae formation is dictated by fusion of the rib tips to the sternum (16), malformation of the sternebrae is likely the result of misalignment of the paired costal cartilages at the point where they fuse to the sternum.

## DISCUSSION

**Paralogous Genes Can Retain Ancestral Functions Yet Also Acquire Additional Activities.** Duplication of *Hox* clusters may have been a prerequisite for increased developmental complexity, allowing at the same time for retention of existing developmental pathways (5, 6). The phenotypic changes common to *Hoxb-8* and *Hoxc-8* transgenic mice primarily affect the vertebrae proper and likely reveal functions once performed by an ancestral group 8 *Hox* gene that have been retained by both paralogs. In addition to the ancestral functions shared by *Hoxb-8* and *Hoxc-8*, these genes appear to perform distinct roles in patterning costal structures, possibly representing entirely new functions that were acquired subsequent to cluster duplication. Loss of function analyses of *Hoxa-3* (17) and *Hoxd-3* (18) as well as *Hoxa-4* (19, 20) and *Hoxb-4* (21) seemed to support the concept of unique functions for paralogs. For example, *Hoxa-3*-deficient mice developed aberrant patterning of neural crest derivatives, while *Hoxd-3*-deficient mice exhibited malformations of skeletal elements derived from axial mesoderm. However, in *Hoxa-3$^{-/-}$/Hoxd-3$^{-/-}$* double-mutant mice, certain aspects of the phenotypes seen in single mutants were exacerbated, suggesting that these paralogs do have partially redundant functions (22).

The alterations in rib morphogenesis induced by *Hoxb-8* and *Hoxc-8* transgenes most likely reflect the exaggeration of functions performed by their endogenous counterparts, since *Hoxc-8* expression appears to be restricted to costal cartilage from 13.5 days p.c. through the time of birth (ref. 23; P. Brulet and L. Tiret, personal communication), while *Hoxb-8* is expressed only in the proximal portion of the rib (Fig. 1 *E* and *F*). It is unlikely that the distinct morphological consequences of altered expression of *Hoxc-8* and *Hoxb-8* can be accounted for by different levels of expression of the two transgenes. The large sample size of independent lines scored for alterations in skeletal morphology makes it likely that a range of transgene

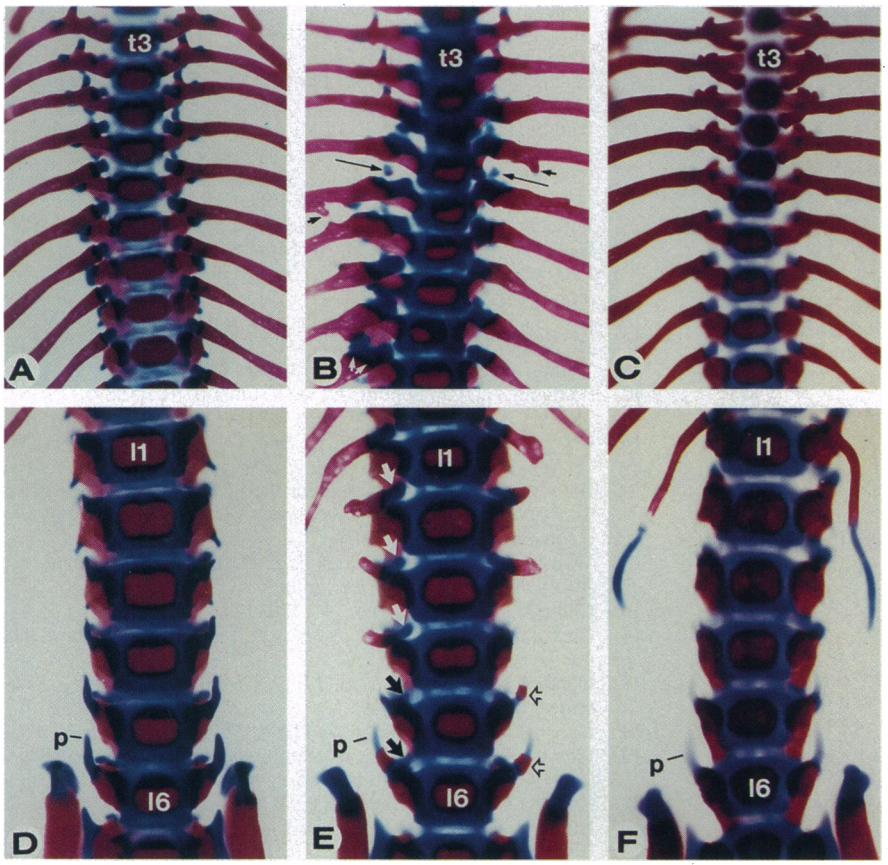


FIG. 3. Ventral views of thoracic and lumbar regions of newborn FVB (*A* and *D*) $Hox^{a\text{-}4}b\text{-}8$ (*B* and *E*) and $Hox^{a\text{-}4}c\text{-}8$ (*C* and *F*) mice. (*B*) Malformations in axial structures are readily apparent in the thoracic region of the $Hox^{a\text{-}4}b\text{-}8$ animal. Note widening of rib heads and proximal ends of rib shafts, forking of the head of the 11th rib (short white arrows), exostoses of rib head cartilage (thin black arrows), knobbing of rib shafts (short black arrows), and malformations of T5 and T10 vertebral centra. FVB (*A*) and $Hox^{a\text{-}4}c\text{-}8$ (*C*) specimens are essentially identical in this view. Ribs are present on the first lumbar vertebrae (l1) of both $Hox^{a\text{-}4}b\text{-}8$ (*E*) and $Hox^{a\text{-}4}c\text{-}8$ (*F*) transgenic newborns. Normal pleurapophyses (p) can be seen in the lumbar region of FVB (*D*) and $Hox^{a\text{-}4}c\text{-}8$ (*F*) mice. An aberrant pattern of ossification (open arrows) can be found in the shaft of many pleurapophyses of $Hox^{a\text{-}4}b\text{-}8$ transgenic mice. Affected pleurapophyses are invariably associated with ectopic cartilage projecting into the intervertebral space (black arrows in *E*). In more severe cases, extensively ossified shafts detach from the neural arch resulting in lumbar ribs that articulate with the vertebrae via cartilaginous heads (white arrows in *E*). t3, Third thoracic vertebra; l6, sixth lumbar vertebra.

expression levels was represented in each case. Furthermore, although the features unique to expression of the $Hox^{a\text{-}4}b\text{-}8$ transgene are visually striking, examination of the alterations common to increased expression of either paralog reveals that the effects of $Hox^{a\text{-}4}c\text{-}8$ expression are more pronounced.

A recent study has described the phenotypic consequences of expressing the *Hoxb-8* gene under the control of the mouse retinoic acid receptor β2 promoter (13). This transgene induced profound alterations in patterning of the forelimbs as well as homeotic transformations in the cervical region of the axial skeleton, including the appearance of ribs or rib heads on C3–C7. The observation of cervical ribs in these mice, taken together with the effects of the $Hox^{a\text{-}4}b\text{-}8$ transgene reported here, strongly implicates the *Hoxb-8* gene in normal rib morphogenesis.

**Atavistic Transformations Induced by *Hoxb-8* and *Hoxc-8*.** Most of the morphologic consequences reported here can be interpreted as the reappearance of ancient patterns. Evolution of tetrapods from rhipidistian fish marked the beginning of a dramatic regionalization of the axial skeleton from a more homogeneous pattern typical of primitive vertebrates. The earliest ribs, complete with heads and independent of the vertebrae, appear in the fossil record from the base of the skull to the tail (24, 25). Although in the transition from reptilian synapsids to early mammals the number of free ribs was dramatically reduced, phylogenetic evidence suggests that vestigial ribs continue to exist in other regions of the vertebral column. For example, the lumbar pleurapophysis most likely represents an ancestral rib that has fused with the lateral portion of the vertebrae and now serves as a point of attachment for muscle groups of the back. The reappearance of free ribs in the $Hox^{a\text{-}4}b\text{-}8$ transgenic mice at the expense of lumbar pleurapophyses is therefore a clear example of atavism.

The presence of a costal tubercle on more posterior ribs in both $Hox^{a\text{-}4}b\text{-}8$ and $Hox^{a\text{-}4}c\text{-}8$ mice is yet another reflection of vertebral history. Ancient tetrapod ribs were invariably bicipital with both heads articulating along the vertebral column. The costal tubercle is an evolutionary vestige of the second head (25), which has been completely lost from lower thoracic ribs in mice.

A third example of atavism induced by increased expression of *Hoxb-8* and *Hoxc-8* involves an intrinsic characteristic of vertebral neural arches. Tetrapod evolution has been marked by acquisition of a stronger, more rigid vertebral column, accomplished largely by development of interlocking zygapophyses on the neural arches (15, 24). In $Hox^{a\text{-}4}b\text{-}8$ and $Hox^{a\text{-}4}c\text{-}8$ mice, the posterior shift in the position of the transitional vertebra has the net effect of lengthening the region governed by the simpler, though less stable, mode of articulation more akin to ancestral forms.

**Evolution of the Vertebrate Body Plan May Be Driven by Repression of *Hox* Gene Function.** Based on their overlapping patterns of expression during mouse embryogenesis, it has been proposed that expression of *Hox* genes forms the basis of positional codes that pattern development of paraxial mesoderm, neuroectoderm, and other embryonic structures (26–28). Models for *Hox* genes in specification of cell identity and in regulating cell proliferation have been proposed (18, 27–29) which predict that the particular complement of *Hox* genes expressed in a developing structure determines its identity (28, 30). This view is supported by the fact that, in mice, vertebrae with similar morphology have similar patterns of *Hox* gene expression and that manipulation of these patterns can partially or wholly alter vertebral identity.

Although an increase in the number of *Hox* genes in the antecedents of vertebrates may have had a dramatic impact on their evolution and subsequent radiation, loss of *Hox* genes has also been suggested to play a role in vertebrate evolution (6). The observation that expansion of the functional domain of a *Hox* gene can result in the transformation of a modern costal structure to a more ancient form suggests that regional repression of *Hox* gene expression could have played a role in the

evolution of the vertebral column. The observation that extending *Hoxb-8* expression into the lumbar region results in the reappearance of costovertebral articulations implies that the development of specialized lumbar ribs could have been due to the reduction in expression or function of a few, perhaps even a single *Hox* gene necessary for the development of rib heads. Similarly, a regional restriction in expression of *Hoxd-4* has been suggested to play a role in evolution of the neocranium from the most anterior vertebrae (31). Since gain of function mutations in *Hoxa-7* (32) and *Hoxc-6* (33) also result in atavistic changes in vertebral morphology, these observations suggest a model in which a major factor in the evolution of a regionalized vertebral column has been regionalization of *Hox* gene function in paraxial mesoderm, a process that may involve both spatial and quantitative changes in *Hox* gene expression. We propose that, in antecedent vertebrates, *Hox* genes involved in patterning the axial skeleton were expressed in relatively broad regions of paraxial mesoderm. The resulting less complex *Hox* code would have established the similar vertebral identities observed in broad regions of early vertebrate skeletons (24, 25). Regionalization of the vertebral column subsequently evolved in concert with the evolution of restricted patterns of *Hox* gene expression in paraxial mesoderm. Spatial restriction most likely involved a shift of the anterior boundaries of mesodermal *Hox* gene expression to distinct, more caudal positions and establishment of posterior boundaries. That null mutations in *Hox* genes can occasionally result in atavistic changes of the axial skeleton (23, 34) can be explained if the elimination of one gene results in an expansion of the domain of function and/or expression of other *Hox* genes and hence generates a more ancient code. Although this may not be a general phenomenon, evidence for cross-regulatory interactions between *Hox* genes both *in vitro* and *in vivo* is mounting (13, 35, 36).

A logical extension of our hypothesis is that further restriction or elimination of *Hox* gene expression may exaggerate an existing evolutionary trend. In fact, the complete loss of function of both *Hoxd-13* (29) and *Hoxa-11* (37) results in incorporation of a fourth vertebra into the sacrum and, in the case of *Hoxa-11*, a reduction in the number of free-rib-bearing vertebrae. Since tetrapod evolution has been marked by the loss of ribs and a gradual increase in the number of sacral vertebrae, from one in amphibians, to two in early reptiles, and to three or more in mammals (24), each of these alterations could be interpreted as a further evolutionary progression through gene loss.

We thank M. Einat, G. Jay, F. Ruddle, M. Utset, and C. Shashikant for comments on the manuscript and helpful discussions. This research was supported by a National Research Service Award fellowship (HD07522) to R.A.P. and a National Institutes of Health grant (HD27943) to C.J.B.

1. McGinnis, W. & Krumlauf, R. (1992) *Cell* **68,** 283–302.
2. Schughart, K., Kappen, C. & Ruddle, F. H. (1989) *Proc. Natl. Acad. Sci. USA* **86,** 7067–7071.
3. Scott, M. P. (1992) *Cell* **71,** 551–553.
4. Kappen, C., Schughart, K. & Ruddle, F. H. (1989) *Proc. Natl. Acad. Sci. USA* **86,** 5459–5463.
5. Ruddle, F. H., Bartels, J. L., Bentley, K. L., Kappen, C., Murtha, M. T. & Pendleton, J. W. (1994) *Annu. Rev. Genet.* **28,** 423–442.
6. Ruddle, F. H., Bentley, K. I., Murtha, M. T. & Risch, N. (1994) *Development (Cambridge, U.K.) Suppl.* **1,** 155–161.
7. Pendleton, J. W., Nagai, B. K., Murtha, M. T. & Ruddle, F. H. (1993) *Proc. Natl. Acad. Sci. USA* **90,** 6300–6304.
8. Pollock, R. A., Jay, G. & Bieberich, C. J. (1992) *Cell* **71,** 911–923.
9. Behringer, R. R., Crotty, D. A., Tennyson, V. M., Brinster, R. L., Palmiter, R. D. & Wolgemuth, D. J. (1993) *Development (Cambridge, U.K.)* **117,** 823–833.
10. Kongsuan, K., Allen, J. & Adams, J. M. (1989) *Nucleic Acids Res.* **17,** 1881–1892.
11. Young, W. S., III (1991) *Focus* **13,** 46–49.
12. Graham, A., Papalopulu, N. & Krumlauf, R. (1989) *Cell* **57,** 367–378.
13. Charite, J., de Graaf, W., Shen, S. & Deschamps, J. (1994) *Cell* **78,** 589–601.
14. Bateson, W. (1894) *Materials for the Study of Variation Treated with Special Regard to Discontinuity in the Origin of Species* (Macmillan, London).
15. Walker, W. F., Jr. (1987) *Functional Anatomy of the Vertebrates: An Evolutionary Perspective* (Saunders, Philadelphia).
16. Chen, J. M. (1953) *J. Anat.* **87,** 130–149.
17. Chisaka, O. & Capecchi, M. R. (1991) *Nature (London)* **350,** 473–479.
18. Condie, B. G. & Capecchi, M. R. (1993) *Development (Cambridge, U.K.)* **119,** 579–595.
19. Kostic, D. & Capecchi, M. R. (1994) *Mech. Dev.* **46,** 231–247.
20. Horan, G. S. B., Wu, K., Wolgemuth, D. J. & Behringer, R. R. (1994) *Proc. Natl. Acad. Sci. USA* **91,** 12644–12648.
21. Ramirez-Solis, R., Zheng, H., Whiting, J., Krumlauf, R. & Bradley, A. (1993) *Cell* **73,** 279–294.
22. Condie, B. G. & Capecchi, M. R. (1994) *Nature (London)* **370,** 304–307.
23. Le Mouellic, H., Lallemand, Y. & Brulet, P. (1992) *Cell* **69,** 251–264.
24. Carroll, R. L. (1988) *Vertebrate Paleontology and Evolution* (Freeman, New York).
25. Hildebrand, M. (1988) *Analysis of Vertebrate Structure* (Wiley, New York), 3rd Ed.
26. Hunt, P., Whiting, J., Muchamore, I., Marshall, H. & Krumlauf, R. (1991) *Development (Cambridge, U.K.) Suppl.* 1, 187–196.
27. Hunt, P. & Krumlauf, R. (1992) *Annu. Rev. Cell. Biol.* **8,** 227–256.
28. Kessel, M. & Gruss, P. (1991) *Cell* **67,** 89–104.
29. Dollé, P., Dierich, A., LeMeur, M., Schimmang, T., Schuhbaur, B., Chambon, P. & Duboule, D. (1993) *Cell* **75,** 431–441.
30. Kessel, M. (1992) *Development (Cambridge, U.K.)* **115,** 487–501.
31. Lufkin, T., Mark, M., Hart, C. P., Dollé, P., LeMeur, M. & Chambon, P. (1992) *Nature (London)* **359,** 835–841.
32. Kessel, M., Balling, R. & Gruss, P. (1990) *Cell* **61,** 301–308.
33. Jegalian, B. G. & De Robertis, E. M. (1992) *Cell* **71,** 901–910.
34. Jeannotte, L., Lemieux, M., Charron, J., Poirier, F. & Robertson, E. J. (1993) *Genes Dev.* **7,** 2085–2096.
35. Zappavigna, V., Renucci, A., Izpisúa-Belmonte, J.-C., Urier, G., Peschle, C. & Duboule, D. (1991) *EMBO J.* **10,** 4177–4187.
36. Zappavigna, V., Sartori, D. & Mavilio, F. (1994) *Genes Dev.* **8,** 732–744.
37. Small, K. M. & Potter, S. S. (1993) *Genes Dev.* **7,** 2318–2328.